



Genes regulating lymphangiogenesis control venous valve formation and maintenance in mice

Eleni Bazigou,¹ Oliver T.A. Lyons,^{2,3} Alberto Smith,² Graham E. Venn,⁴ Celia Cope,³ Nigel A. Brown,³ and Taija Makinen¹

¹Lymphatic Development Laboratory, Cancer Research UK London Research Institute, London, United Kingdom. ²Academic Department of Surgery, Cardiovascular Division, Kings College London, BHF Centre of Research Excellence and NIHR Biomedical Research Centre at King's Health Partners, St Thomas' Hospital, London, United Kingdom. ³Division of Biomedical Sciences, St George's, University of London, Cranmer Terrace, London, United Kingdom. ⁴Cardiothoracic Surgery, St Thomas' Hospital, King's Health Partners, London, United Kingdom.

Chronic venous disease and venous hypertension are common consequences of valve insufficiency, yet the molecular mechanisms regulating the formation and maintenance of venous valves have not been studied. Here, we provide what we believe to be the first description of venous valve morphogenesis and identify signaling pathways required for the process. The initial stages of valve development were found to involve induction of ephrin-B2, a key marker of arterial identity, by venous endothelial cells. Intriguingly, developing and mature venous valves also expressed a repertoire of proteins, including prospero-related homeobox 1 (Prox1), Vegfr3, and integrin- α 9, previously characterized as specific and critical regulators of lymphangiogenesis. Using global and venous valve-selective knockout mice, we further demonstrate the requirement of ephrin-B2 and integrin- α 9 signaling for the development and maintenance of venous valves. Our findings therefore identified molecular regulators of venous valve development and maintenance and highlighted the involvement of common morphogenetic processes and signaling pathways in controlling valve formation in veins and lymphatic vessels. Unexpectedly, we found that venous valve endothelial cells closely resemble lymphatic (valve) endothelia at the molecular level, suggesting plasticity in the ability of a terminally differentiated endothelial cell to take on a different phenotypic identity.

Introduction

Luminal valves are required in the heart, veins, and lymphatic vessels to ensure unidirectional flow of blood and lymph. In addition, specialized intraluminal valves at the connections of the subclavian veins and the thoracic and right lymphatic ducts facilitate 1-way transport of lymph into the venous circulation and thus ensure the functionality of the entire lymphatic system (1). Valves operate under different pressures and flow rates depending on their location along the vascular tree. These differences are mirrored in their distinct morphological features. For example, both heart and lymphatic valves are composed of endothelial-lined leaflets with a connective tissue core, but only the former also contain a muscular component and valvular interstitial cells that are responsible for the synthesis, remodeling, and repair of the valve matrix (2).

The molecular mechanisms regulating the morphogenesis of heart valves have been extensively studied, as dysfunction of these valves has obvious clinical implications (2). In addition, regulators of lymphatic valve development, including the forkhead transcription factor *Foxc2*, the transmembrane ephrin-B2 ligand, and the cell matrix adhesion receptor integrin- α 9, have recently been identified (3–5). Analysis of respective knockout mouse models has further provided insight into the morphogenesis and physiological importance of lymphatic valves (3, 4, 6). Compared with cardiac and lymphatic valves, the mechanisms regulating venous valves are

poorly understood, yet dysfunction of venous valves also leads to clinical disease. Congenital or acquired failure of the venous calf pump, for example, results in venous hypertension, leading to skin damage and chronic ulceration that may be treatment resistant. Valve incompetence (reflux) is also a major feature of varicose veins (7). Better understanding of the factors regulating venous valve development should allow the identification of those at risk for venous hypertension and enable preventive and novel therapies.

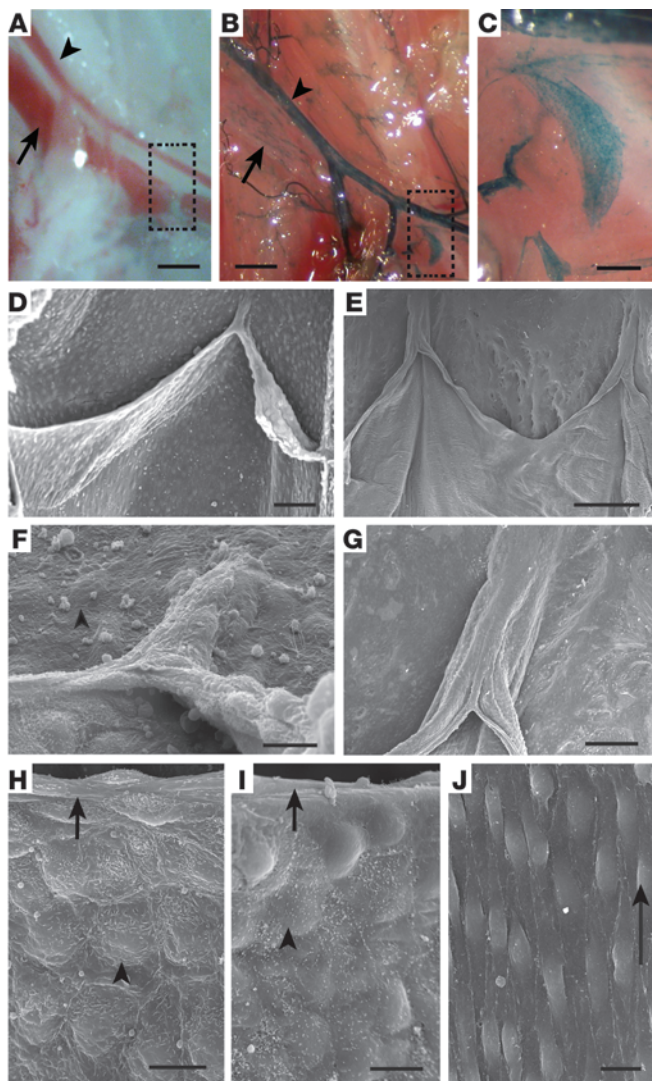
In humans, mutations in *FOXC2* have been identified as the cause of lymphoedema distichiasis (LD) (8). Studies in LD patients and *Foxc2*-deficient mouse mutants indicate that the underlying cause for lymphatic failure in LD is abnormal valve morphogenesis (5, 6). Patients with LD, and all their relatives who carry *FOXC2* mutations but do not have clinical LD, have long saphenous vein reflux, supporting a role for *FOXC2* in venous valve development (9). In lymphatic valves, *Foxc2* acts together with NFATc1 (6), a regulator of cardiac valve development (10), and cooperates with VEGFR3 signaling (5, 6). Mutations in *VEGFR3* cause lymphatic dysfunction in Milroy disease, the most common form of congenital lymphoedema, and the majority of Milroy patients also have reflux in the great saphenous vein (11). These findings suggest that *Foxc2*-NFATc1-VEGFR3 signaling may regulate the development of valves in different vessel types; however, this has not been directly investigated because of the lack of methods and genetic models to study venous valves.

Here, we have developed methods to visualize and genetically target venous valves in mice. We showed that the morphogenetic process of valve development occurred similarly in veins and lymphatic vessels and was regulated via common molecular mecha-

Authorship note: Eleni Bazigou and Oliver T.A. Lyons contributed equally to this work.

Conflict of interest: The authors have declared that no conflict of interest exists.

Citation for this article: *J Clin Invest.* 2011;121(8):2984–2992. doi:10.1172/JCI58050.

**Figure 1**

Characterization of venous valves in mice and humans. (A–C) Stereomicroscopic visualization of murine valves in the iliac veins. The boxed region in A was photographed after X-gal staining in a *Tie2^{lacZ}* reporter mouse (B) to visualize the valve leaflets (C). Arrow, vein; arrowhead, artery. (D–J) SEM images of the lumen of mouse (D, F, H, and J; $n = 24$) and human (E, G, and I; $n = 4$) veins, showing the overall valve structure (D and E), commissure (F and G), valve leaflet (H and I), and vessel wall upstream of the valve (J). (H, I, and F) Arrowheads denote a round endothelial cell on the leaflet (H and I) or downstream of the valve (F); arrows denote fusiform cells forming the free edge of the leaflet. The arrow in J shows the direction of flow. Scale bars: 1 mm (A, B, and E); 250 μm (C); 125 μm (D); 10 μm (F and H–J); 250 μm (G).

sis was carried out on human venous valves (Figure 1E). The free edges of the valve leaflets fused shortly before insertion into the vessel wall at the commissure (Figure 1, F and G). SEM analysis also showed that the edges of valve leaflets were lined by transversely aligned fusiform cells, while the cells on the leaflet and downstream on the outflow side of the valve had a rounded morphology (Figure 1, F, H, and I). In contrast, endothelial cells located upstream on the inflow side of the valve aligned in the direction of blood flow (Figure 1J). Similar cell arrangement was observed around lymphatic valves (Supplemental Figure 1, A–C; supplemental material available online with this article; doi:10.1172/JCI58050DS1), whereas endothelial cells of lymphatic capillaries that were exposed to low fluid shear forces were not aligned (Supplemental Figure 1, D and E). The shared morphological features between mice and humans demonstrated the suitability of the mouse as a model for studying human venous valve pathology.

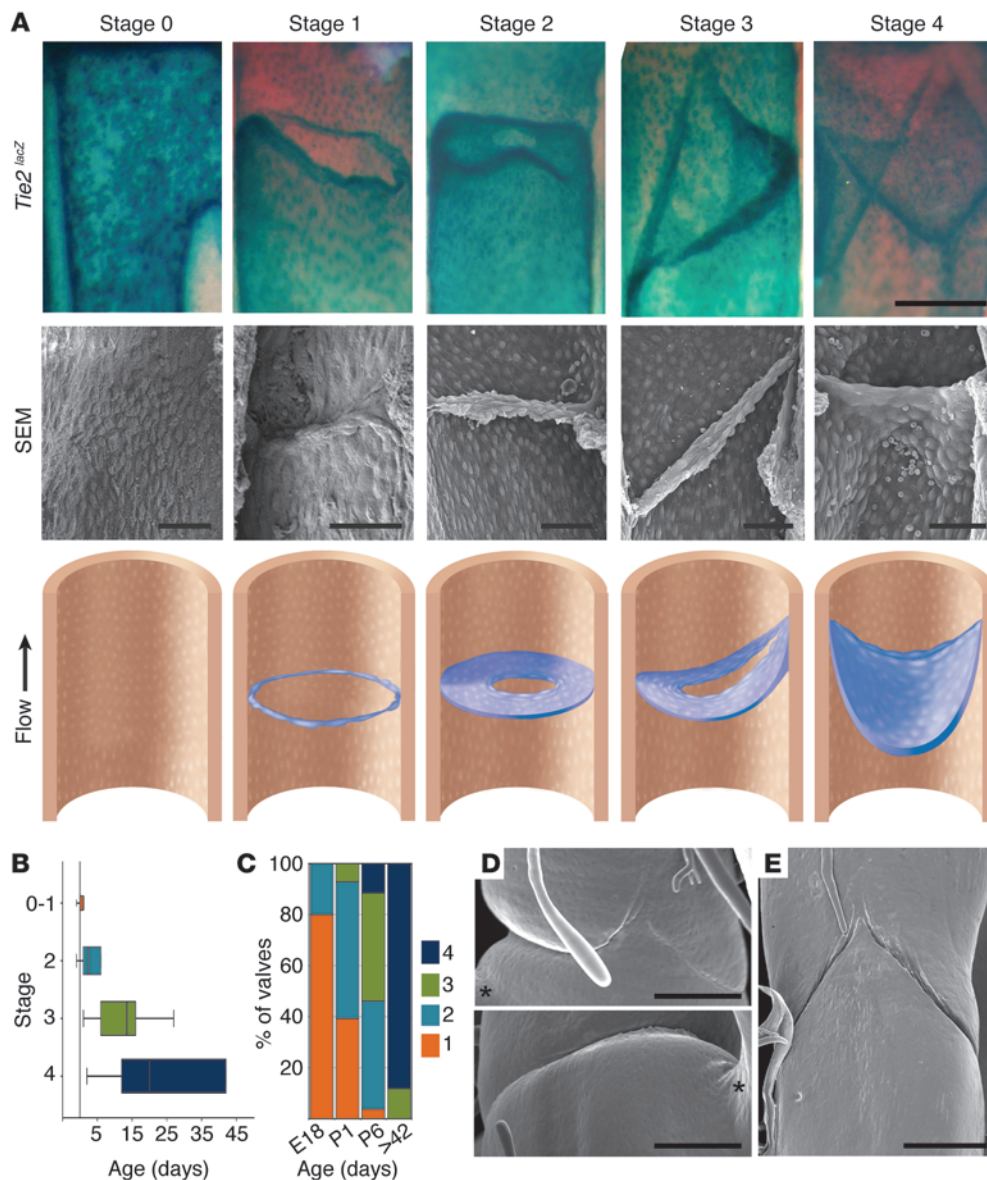
Characterization of venous valve development. Venous valve development in *Tie2^{lacZ}* mice of different developmental stages was assessed by staining for β -gal reporter activity and by SEM imaging (Figure 2A). Formation of valves in external iliac veins was initiated at E18, when a distinct region of cells rounded up and altered their alignment at the site of the developing valve (stage 0). The endothelial cells subsequently acquired transverse polarity and were aligned, in a ring, perpendicular to the longitudinal axis of the vein (stage 1). Formation of the leaflets occurred postnatally (Figure 2, A–C). The initial stages of valve development correlated with the formation of a boundary in β -gal stain, with increased staining observed upstream of the developing valve (Figure 2A). Development proceeded in clear stages, beginning with ingrowth of a circumferential shelf, which produced marked luminal constriction (stage 2). The subsequent formation of one commissure (stage 3) was later followed by the second commissure (stage 4). This morphological progression was confirmed by quantifying the valve stages in animals of different ages (Figure 2, B and C). There was variation in the progression of valve formation, and valves were often observed at different stages of development on either side of the same animal. A small proportion of valves appeared to remain at a single commissure stage (i.e., stage 3) in adult mice (Figure 2C). This morphology was also identified in an adult mouse by SEM analysis of a resin cast, but most adult valves had 2 commissures (Figure 2, D and E, and data not shown).

Venous valves express markers of arterial and lymphatic endothelia. Recent studies have revealed several molecules that are required for lymphatic valve development, including ephrin-B2, integrin- $\alpha 9$, and its ligand, fibronectin, containing an alternatively spliced EIIIA domain (Fn-EIIIA) (3, 4). Expression of these molecules was

nisms involving integrin- $\alpha 9$ and ephrin-B2 signaling. Collectively, our results suggest that valve endothelial cells possess a unique identity independent of the type of vessel in which it develops, but likely attributed to the function of the luminal valve.

Results

Mouse and human venous valves share common morphological features. We first established methodology for venous valve visualization in the mouse. Stereomicroscopic examination of the region of the femoral and external iliac vein revealed the presence of a valve distal to the origin of the common iliac vein (Figure 1A). Characterization of the vessels and valves using mice expressing β -gal under the control of the *Tie2* gene promoter (12) together with whole-mount X-gal staining revealed prominent β -gal expression in the arterial endothelia, with weaker and patchy staining in the veins (Figure 1B). In contrast, venous valves stained strongly for β -gal activity (Figure 1, B and C). Murine valves were found to be bicuspid and frequently occurred near a tributary (Figure 1A and data not shown). Endothelial cell shapes and arrangement within the valve were imaged using scanning electron microscopy (SEM) after a longitudinal incision was made along the length of the vessel (Figure 1D). A similar analy-



therefore examined in the valves of the external iliac veins using immunofluorescence. Integrin- $\alpha 9$ and Fn-EIIIA were specifically expressed in the developing venous valves in early postnatal mice (Figure 3, A, B, D, E, G, and H). Integrin- $\alpha 9$ was also expressed in adult valves (data not shown). Expression of ephrin-B2 was assessed using a GFP reporter mouse (13). Strong *Efnb2* promoter-driven nuclear GFP expression was found in the endothelial cells of the venous valve both during valvulogenesis and in adulthood, with weaker expression on the venous wall downstream of the developing valve (Figure 3, A, C, J, and K).

The molecular identity of venous valve endothelial cells was further characterized by examining the expression of prospero-related homeobox 1 (*Prox1*) and *Vegfr3*, 2 major regulators of lymphangiogenesis that are highly expressed in lymphatic valves (6). Immunofluorescence staining revealed strong and specific expression of *Prox1* in the endothelial cells of developing and mature murine venous valves (Figure 3, D, F, J, and K). *PROX1* was also expressed in human venous valves (Figure 3, M and N). Whereas most

valve endothelial cells expressed ephrin-B2, as assessed by *Efnb2^{GFP}* fluorescence, the cells on the free edges of the leaflets expressing the highest levels of *Prox1* were *Efnb2^{GFP}*-negative (Figure 3, J and K). *VEGFR3* expression, visualized using a *lacZ* reporter, was observed in developing, but not adult, venous valves (Figure 3, I and L). These expression data suggest a unique identity of valve endothelial cells: unlike other venous endothelial cells, the valve endothelial cells express several well-characterized markers of lymphatic (*Prox1*, *Vegfr3*, and integrin- $\alpha 9$) or arterial and lymphatic (ephrin-B2) endothelia, which are also strongly expressed in lymphatic valves.

Prox1 expression in developing and mature venous valves allows genetic targeting of valve endothelial cells in *Prox1-CreER^{T2}* mice. In order to investigate the function of candidate genes specifically in venous valves, we generated a transgenic mouse line expressing tamoxifen-inducible Cre recombinase (*CreER^{T2}*) under the control of the *Prox1* gene promoter. The efficiency and specificity of the *Prox1-CreER^{T2}* line was examined by crossing this line with the *R26-mTmG* reporter (14), followed by administration of 4-hydroxy-

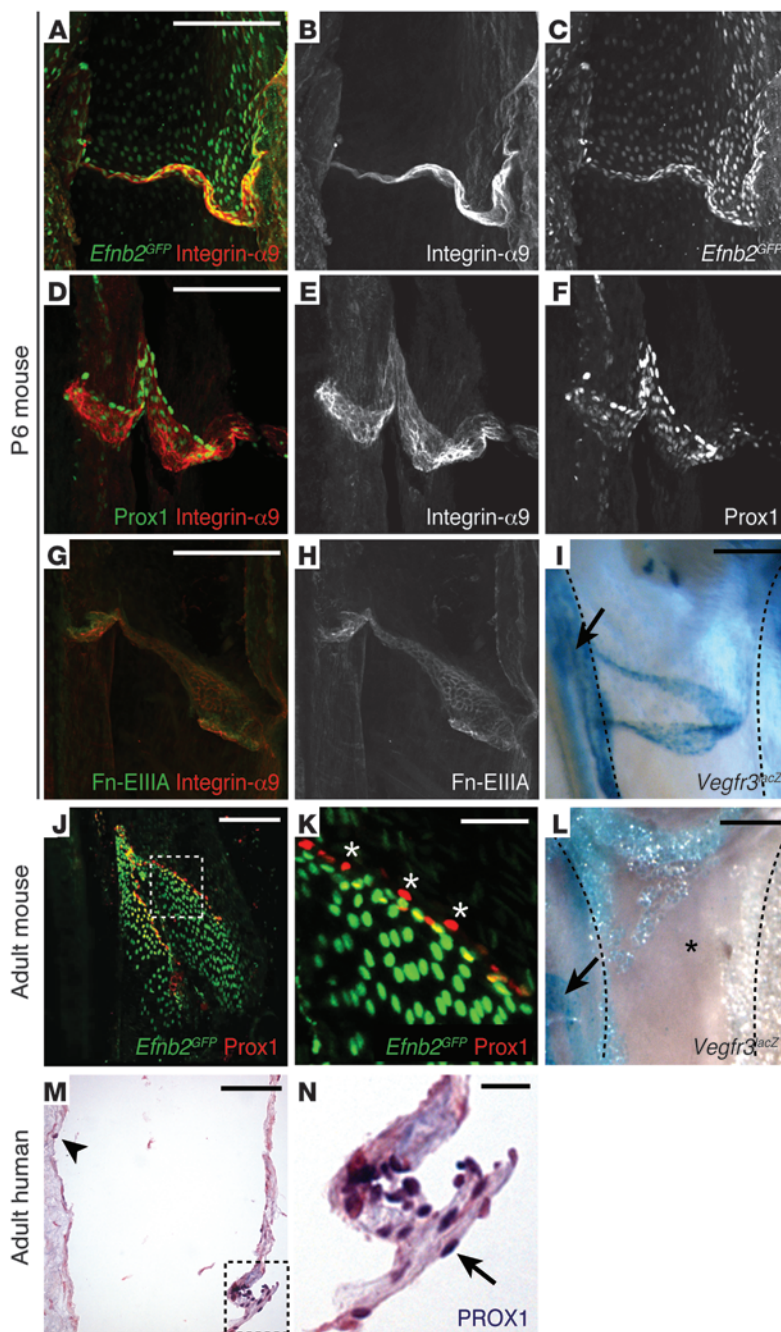


Figure 3

Unique molecular identity of venous valve endothelial cells. (A–L) Immunofluorescence staining of murine venous valves using antibodies against integrin- $\alpha 9$ (A, B, D, E, and G), Prox1 (D, F, J, and K), and Fn-EIIIA (G and H) at the indicated stages. Visualization of ephrin-B2 and Vegfr3 expression was achieved using reporter mice expressing nuclear GFP (*Efnb2^{GFP}*; A, C, J, and K) or β -gal (*Vegfr3^{lacZ}*; I and L), respectively. (K) Higher-magnification view of the boxed region in J. Note high expression of Prox1 in ephrin-B2-negative cells on the free edges of valve leaflets (asterisk). (I and L) *Vegfr3^{lacZ}* reporter activity was present in developing (I) but not in adult (L; asterisk) valves. Arrows denote an adjacent lymphatic vessel; dotted lines outline the iliac vein. (M and N) Immunostaining of adult human venous valve using antibodies against PROX1. (N) Higher-magnification view of the boxed region in M. Arrow denotes a Prox1-positive (dark blue) endothelial cell on the free edge of the valve leaflet; arrowhead denotes a cell on the wall of the vein. Scale bars: 50 μ m (A–J and L); 20 μ m (K and N); 100 μ m (M).

mice at P0 led to Cre-mediated recombination in a subset of venous endothelial cells (data not shown). The targeted cells were not found in specific locations along the vein; instead, there was widespread GFP labeling of the valve and the adjacent vessel wall when the tissue was analyzed at P7 (Figure 4D). In contrast to *Prox1* promoter-driven reporter gene activity, *Prox1* protein expression was undetectable in the veins at P0, although the sites of developing valves were visualized at P0 by GFP expression driven by the *Efnb2* promoter (Figure 4, E and F), which suggests that the earliest stages of valve development involve induction of *Efnb2* expression. 4-OHT treatment of *R26-mTmG;Prox1-CreER^{T2}* mice at P2 resulted in efficient and more selective labeling of venous valve endothelial cells at P7, which correlated with strong expression of *Prox1* protein in developing venous valves at P2 (Figure 4, G–I). Administration of tamoxifen to adult *R26-mTmG;Prox1-CreER^{T2}* mice similarly led to efficient Cre-mediated recombination and activation of GFP expression in venous valves and lymphatic vessels after 1 week of treatment (Figure 4, J and K).

These findings demonstrated the suitability of the *Prox1-CreER^{T2}* line for targeting venous valves during development and in adults. The data on protein expression and promoter activity also suggest that *Prox1* is expressed widely, but at low levels, in the iliac veins during early postnatal development and is strongly upregulated upon initiation of valve formation.

Valve-selective deletion of integrin- $\alpha 9$ and ephrin-B2 disrupt venous valve morphogenesis. Lack of ephrin-B2 or integrin- $\alpha 9$ signaling leads to failure of lymphatic valve morphogenesis, characterized by valve leaflet formation that is, respectively, absent or rudimentary (3, 4). The functional importance of these genes in venous valve development was examined using global knockout mice for integrin- $\alpha 9$ and its ligand, Fn-EIIIA, and by generating valve-selective deletions of integrin- $\alpha 9$ and ephrin-B2 by crossing mice carrying floxed alleles with the *Prox1-CreER^{T2}* animals.

tamoxifen (4-OHT) and analysis of reporter gene expression. Intraperitoneal injection of 4-OHT resulted in efficient Cre-mediated GFP expression in the lymphatic vasculature and in other *Prox1*-expressing tissues, such as heart and liver (Figure 4, A and B, and data not shown). No GFP fluorescence was observed in the dermal blood vessels, but, consistent with the expression of *Prox1* in venous valve endothelial cells (Figure 3, D and J), GFP⁺ valves were found in the iliac veins (Figure 4, A–C).

A time course analysis in which 4-OHT was administered at different postnatal stages was carried out in order to assess the earliest stage at which *Prox1* promoter was active during venous valve development. 4-OHT injection of *R26-mTmG;Prox1-CreER^{T2}*

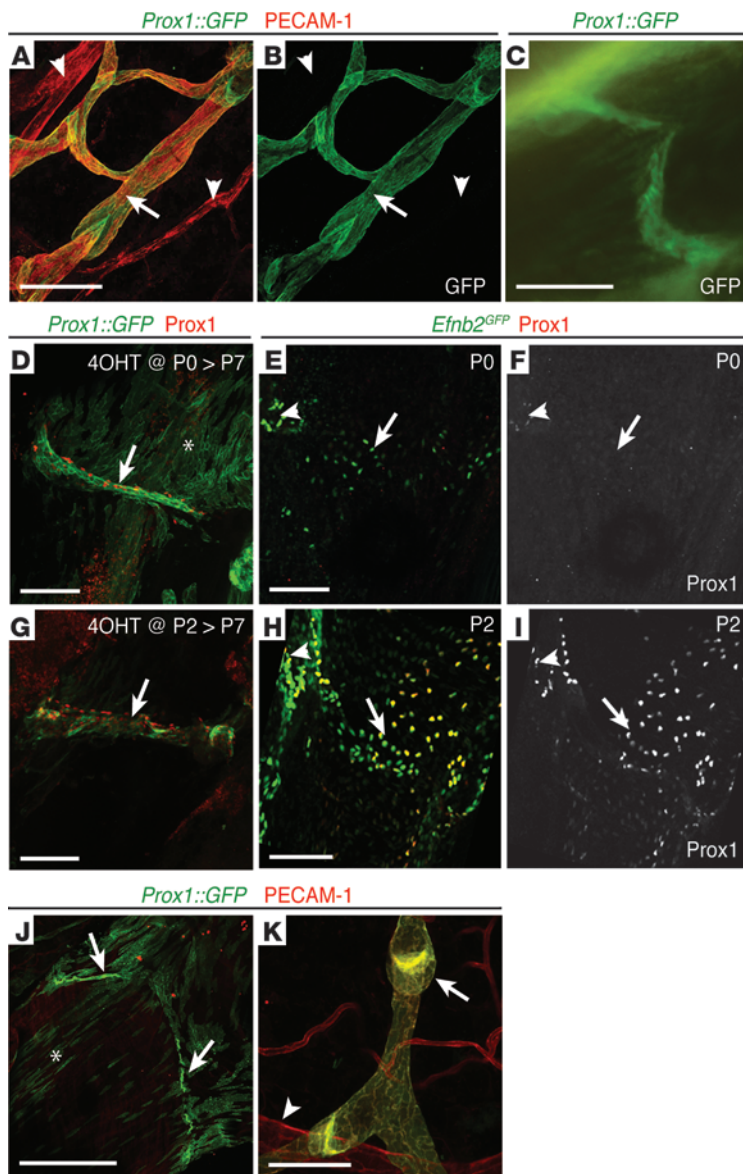


Figure 4

Prox1 expression in developing and mature venous valves allows genetic targeting of valve endothelial cells in *Prox1-CreER^{T2}* mice. (A and B) Immunofluorescence of ear skin from 3-week-old *R26-mTmG;Prox1-CreER^{T2}* (*Prox1::GFP*) mouse administered 4-OHT at P1. Arrow, lymphatic vessel (GFP⁺PECAM-1⁺); arrowhead, blood vessel (GFP⁺PECAM-1⁻). (C) Expression of GFP in venous valve of P7 *R26-mTmG;Prox1-CreER^{T2}* mouse administered 4-OHT at P1. (D–I) Immunofluorescence staining of iliac veins of *R26-mTmG;Prox1-CreER^{T2}* (D and G) and *Efnb2^{GFP}* (E, F, H, and I) mice at the indicated times using Prox1 antibodies (red). Note GFP expression in the developing valve (arrow) and in vessel wall (asterisk) in *R26-mTmG;Prox1-CreER^{T2}* mice after 4-OHT treatment at P0 (D), but more restricted expression in the valve after treatment at P2 (G, arrow). (E, F, H, and I) Arrows, developing venous valves; arrowheads, adjacent lymphatic vessels. (J and K) Immunofluorescence of iliac vein (J) and ear skin (K) from a 4-week-old *R26-mTmG;Prox1-CreER^{T2}* mouse fed tamoxifen-containing diet for 2 weeks. (J) Arrows, GFP⁺ cells on the free edges of valve leaflets; asterisk, recombination in some individual endothelial cells on the vein wall. (K) Arrow, lymphatic vessel (GFP⁺PECAM-1⁺); arrowhead, blood vessel (GFP⁺PECAM-1⁻). Scale bars: 50 μm (A–I and K); 300 μm (J).

onstrated tissue-autonomous requirement for integrin-α9 in valve-forming cells. A similar phenotype was observed in *Fn-III^A*^{-/-} mice, although with lower penetrance (Figure 5E; 4 of 8 valves analyzed; *P* < 0.05, Fisher exact test), which suggests the involvement of additional integrin-α9 ligands.

Similar to integrin-α9 signaling, valve-selective deletion of ephrin-B2 in veins recapitulated the phenotype previously reported in lymphatic valves. *Efnb2^{lox/lox};Prox1-CreER^{T2}* mice administered 4-OHT at P2 showed defective venous valves, characterized by absent or short leaflets at P11 (Figure 5F; 10 of 10 valves analyzed; *P* < 0.01, Fisher exact test). Whereas Prox1-positive valve leaflets were visualized in the veins of control and *Itga9*-deficient mice, no Prox1-positive cells were detected in *Efnb2*-deficient veins (Figure 5, G–L).

Collectively, these data suggest that both integrin-α9 and ephrin-B2 are important regulators of venous valve development. Given their previously demonstrated roles in lymphatic valve morphogenesis, these findings further suggest that common molecular mechanisms regulate the development of valves in the 2 vessel types.

Differential requirement of integrin-α9 and ephrin-B2 in the maintenance of venous and lymphatic valves. To examine the effect of integrin-α9 and ephrin-B2 signaling on valve maintenance, we deleted these genes at later postnatal stages, when the development of venous valves has been completed. Feeding 3-week-old *Itga9^{lox/lox};Prox1-CreER^{T2}* and *Efnb2^{lox/lox};Prox1-CreER^{T2}* mice tamoxifen-containing diet for 2 weeks led to efficient Cre-mediated deletion in venous valve endothelial cells (Figure 4J and data not shown). Compared with control valves, *Itga9* and *Efnb2* mutants showed regression of the valve leaflet, such that only a remnant remained at the junction of the leaflet and vessel wall (Figure 6, A–F).

To address whether the 2 genes are similarly required for maintenance of mature lymphatic valves, we analyzed the dermal lymphatic vessels in the ears of adult mice using immunofluorescence. Compared with controls, *Itga9^{lox/lox};Prox1-CreER^{T2}* mice showed

Itga9 deficiency causes early postnatal lethality (15). Valve development in these mice was therefore examined at P6. At this stage, most littermate controls had developed venous valves with elongated leaflets and at least 1 commissure (Figure 5A; 7 of 10 valves analyzed; see also Figure 2C). In contrast, SEM analysis of *Itga9*^{-/-} valves showed hypoplastic leaflets (Figure 5B; 4 of 5 valves analyzed), similar to the defect previously reported in lymphatic valves (3). Even the most severely affected valves contained cells that were oriented perpendicular to the direction of flow (Figure 5B and data not shown), which suggests that the initial stages of valve development occurred normally. Conditional deletion of integrin-α9 postnatally using *Prox1-CreER^{T2}* mice circumvented lethality and allowed us to analyze valves in older mice at P11, when all control mice showed well-developed valve leaflets (Figure 5C; 10 valves analyzed). Administration of 4-OHT to *Itga9^{lox/lox};Prox1-CreER^{T2}* mice at P2 resulted in hypoplastic venous valve leaflets at P11 (Figure 5D; 6 of 7 valves analyzed; *P* < 0.01, Fisher exact test) in the absence of lymphatic vascular defects (Supplemental Figure 2, A and B). This recapitulated the knockout phenotype and dem-

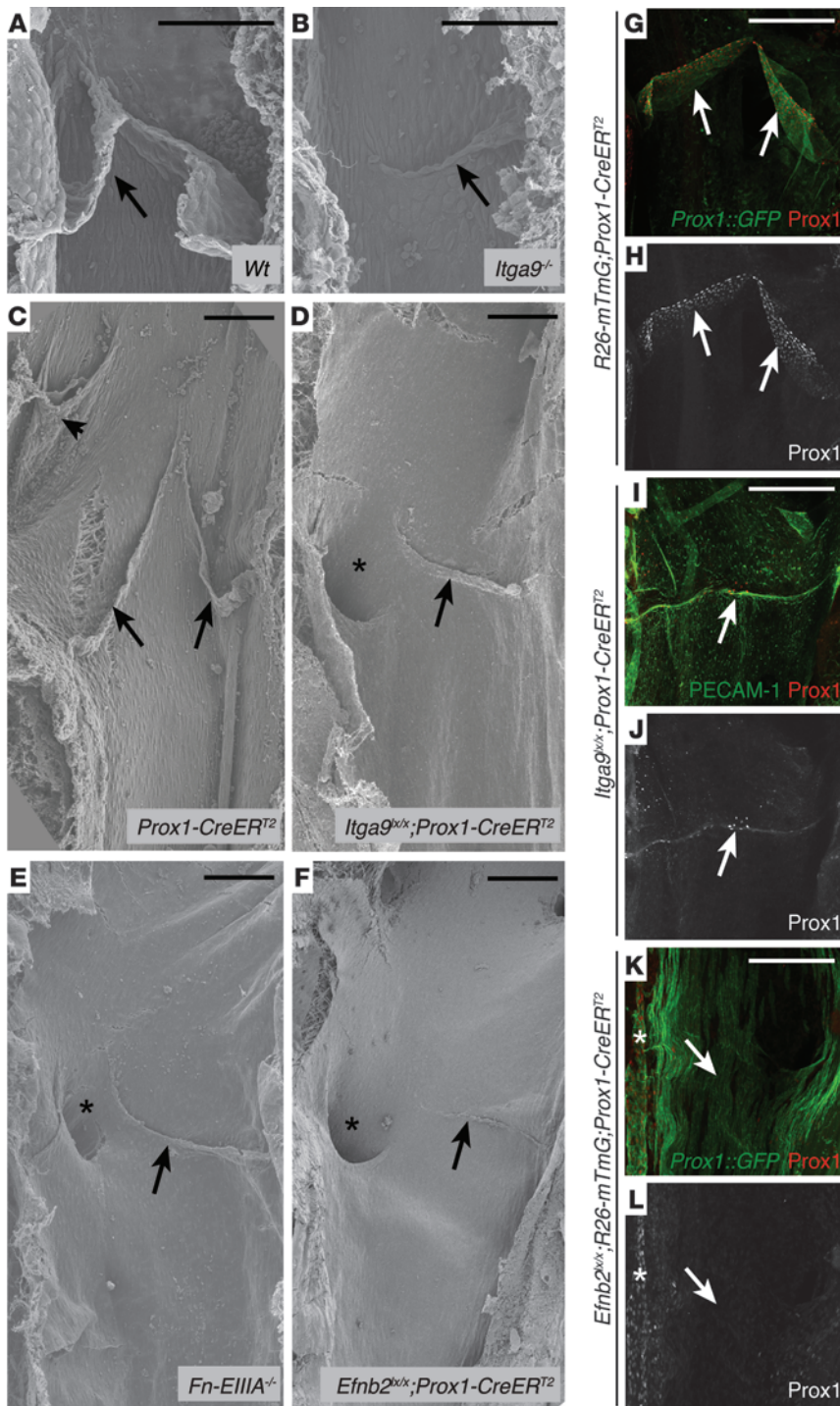


Figure 5
 Integrin- $\alpha 9$ and ephrin-B2 are required for the development of venous valves. (**A** and **B**) SEM images of venous valves (arrows) in P6 WT (**A**) and *Itga9*^{-/-} (**B**; 5 valves) mice. (**C–F**) SEM images of venous valves in control (**C**; 10 valves), *Itga9*^{lox/+};*Prox1-CreER*^{T2} (**D**; 7 valves), *Fn-ElIIIA*^{-/-} (**E**; 8 valves), and *Efnb2*^{lox/+};*Prox1-CreER*^{T2} (**F**; 10 valves) mice at P11. Arrows, valves in external iliac veins; arrowheads, valves in internal iliac veins. Note the rudimentary valves in the external iliac vein and absent valves (asterisks) in the internal iliac vein in the mutant mice. (**G–L**) Immunofluorescence staining of iliac veins of *R26-mTmG*;*Prox1-CreER*^{T2} (**G** and **H**), *Itga9*^{lox/+};*Prox1-CreER*^{T2} (**I** and **J**; *n* = 2), and *Efnb2*^{lox/+};*R26-mTmG*;*Prox1-CreER*^{T2} (**K** and **L**; *n* = 3) mice at P7, after administration of 4-OHT at P2, using an antibody against Prox1 (red). PECAM-1 antibodies were used to visualize endothelial cells in **I**. Note the endothelial cells on the free ends of the valve leaflets (arrows) showed colocalization of GFP and strong Prox1 immunolabeling (**G** and **H**), reduced number of Prox1-positive cells in *Itga9* mutants (**I** and **J**), and loss of Prox1-positive cells in *Efnb2* mutants (**K** and **L**). Asterisks in **K** and **L** denote a lymphatic vessel. Scale bars: 100 μ m.

sels (Supplemental Figure 2, A–C). These data demonstrated a continuous requirement of integrin- $\alpha 9$ and ephrin-B2 signaling for the maintenance of venous valves. Ephrin-B2, but not integrin- $\alpha 9$, was additionally required for the maintenance of lymphatic valves.

Discussion

The clinical problems that arise from venous valve incompetence highlight the importance of valves in ensuring unidirectional flow and efficient return of blood, especially from the lower extremities. However, the mechanisms that regulate venous valve development have not been described. In the present study, we used genetic reporter strains, SEM, and whole-mount immunofluorescence to characterize the morphology and development of murine venous valves. Valve development was initiated by endothelial cell reorientation followed by ingrowth to form a circumferential shelf, then development of first one and then a second commissure. Notably, the first anatomical description of venous valve development

apparently normal lymphatic vasculature after 2 weeks of tamoxifen treatment, in spite of depletion of integrin- $\alpha 9$ protein (Figure 6, G–J, M, and N). However, there was a small reduction in the number of valves (Figure 6O). In contrast, deletion of *Efnb2* in mature lymphatic valves led to a significant reduction in their number, and the remaining valves showed an abnormal morphology (Figure 6, K, L, and O). Similar observations were made from analyses of mesenteric lymphatic vessels at P7 after 4-OHT treatment at P2, when fully developed valves were already present in these ves-

by Kampmeier in the early 20th century accurately captured the basic morphogenic events (16). The process of valve development described in the present study is also comparable to our previous description of lymphatic valve formation (3), with the exception that we did not previously describe the single commissure stage.

SEM analyses of mouse and human venous valves revealed morphological differences between the endothelial cells in different parts of the vessel. We found that the cells located upstream of the valve were elongated and aligned in the direction of flow,

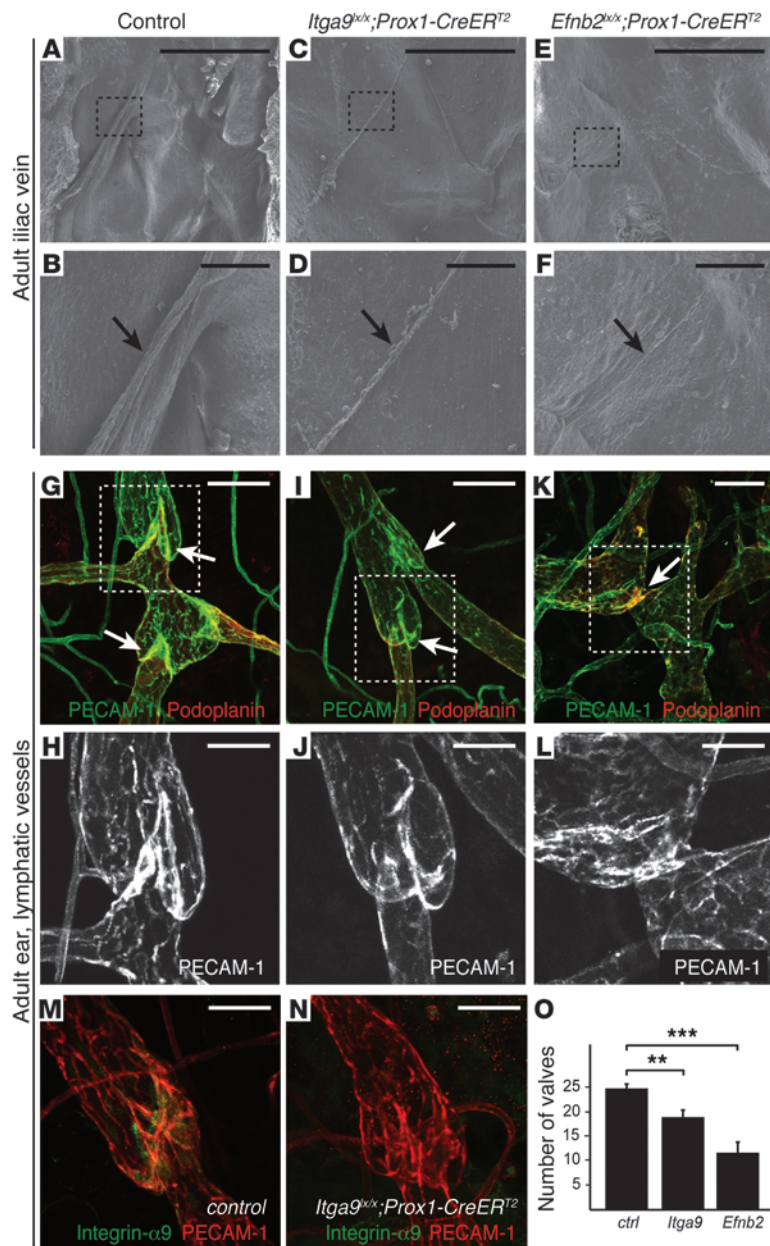


Figure 6

Differential requirement of integrin- α 9 and ephrin-B2 for the maintenance of venous and lymphatic valves. (A–F) SEM images of venous valves of adult control and *Itga9* and *Efnb2* mutant mice (3 valves per genotype) after oral administration of tamoxifen for 2 weeks. (B, D, and F) Higher-magnification views of the boxed regions in A, C, and E, respectively. Arrows denote valve leaflets. (G–L) Immunofluorescence of ears of control *Prox1-CreER^{T2}* (G and H), *Itga9^{lox/+};Prox1-CreER^{T2}* (I and J) and *Efnb2^{lox/+};Prox1-CreER^{T2}* (K and L) adult mice ($n = 3$ per genotype) using antibodies against PECAM-1 (green) and podoplanin (red). Arrows denote valves. (H, J, and L) Higher-magnification views of boxed regions in G, I, and K, respectively. (M and N) Immunofluorescence of ears of control *Prox1-CreER^{T2}* (M) and *Itga9^{lox/+};Prox1-CreER^{T2}* (N) adult mice after oral administration of tamoxifen for 2 weeks, using antibodies against PECAM-1 (red) and integrin- α 9 (green). Note the reduced expression of integrin- α 9 in the *Itga9* mutants. (O) Number of lymphatic valves in the ear skin of adult control and *Itga9* and *Efnb2* mutant mice. Data represent mean \pm SD valves in 0.5-mm² dermal area ($n = 3$ per genotype, 2 random areas per mouse). ** $P = 0.005$, *** $P < 0.001$, t test. Scale bars: 500 μ m (A, C, and E); 50 μ m (B, D, F, G, I, and K); 20 μ m (H, J, L, M, and N).

expression and actin cytoskeleton (21). Interestingly, we observed a boundary in β -gal staining in the *Tie2^{lacZ}* mice and induction of *Efnb2^{GFP}* reporter activity concomitant with the early stages of valve formation. This could be related to the flow patterns around the developing valve that may be involved in establishing its gene expression profile and structure. Exposure of cultured cells to shear stress in vitro leads to upregulation and phosphorylation of Tie2 (22, 23). In addition, expression of angiopoietin-2, an antagonistic Tie2 ligand, is downregulated under shear stress (23), which suggests that Tie2-mediated signaling may be involved in regulating endothelial cell responses to flow.

Gene expression analyses revealed that several genes that are highly expressed in lymphatic valves were also present in venous valves; these included *Itga9*, *Prox1*, and *Vegfr3*. Notably, these 3 genes have previously been characterized as lymphatic-specific markers and critical regulators of lymphangiogenesis (3, 24, 25), with the exception of *Vegfr3*, which is also

expressed in fenestrated and newly formed blood vessels and regulates angiogenesis (25–27). In particular, expression of *Prox1* in venous valves is surprising, given its well-established role as the master regulator of lymphatic endothelial cell fate (24, 28). Unexpectedly, specific expression of ephrin-B2, a key arterial and lymphatic marker (4, 29), was also found in the venous valves. In fact, induction of *Efnb2* expression by venous endothelial cells represented one of the earliest stages in valve development. These expression data suggest that valve endothelial cells have a unique identity that is likely attributed to the function of the valve rather than to the type of vessel in which it develops. Furthermore, our findings suggest that venous endothelial cells exhibit plasticity in their ability to take on a different phenotypic identity, thus challenging the common view that endothelial cells in different types of vessels represent distinct terminally differentiated cell

whereas the cells on the leaflet and downstream of the valve had a rounded morphology, as previously described in venules (17). A similar arrangement of cells was observed in lymphatic valves. Such differences likely arise from differential exposure to fluid shear stress, which suggests that flow patterns are involved in modulating endothelial cell phenotypes within the valve. In agreement with this suggestion, endothelial cells of lymphatic capillaries exposed to low shear stress levels showed no alignment, whereas cells of the thoracic duct, the largest lymphatic vessel, were aligned in the direction of flow. Previous studies have shown the involvement of shear stress generated by flowing blood in patterning the developing vasculature by, for example, regulating branching morphogenesis and asymmetric remodeling of the aortic arches (18–20). At the cellular level, flow-induced endothelial responses include instantaneous ion fluxes as well as signaling cascades that lead to changes in gene



lineages whose identity is strictly genetically determined. The importance of environmental cues in regulating endothelial cell identities was previously highlighted by the observation that arterial and venous identities could be altered by changing the flow conditions in the vessels (19).

Generation of a mouse line expressing tamoxifen-inducible Cre recombinase under the control of the *Prox1* promoter allowed us to target endothelial cells of both developing and mature venous valves. Integrin- $\alpha 9$ and ephrin-B2, the previously identified regulators of lymphatic valve development, were required for venous valve morphogenesis. We believe our study establishes these 2 genes as the first-described regulators of this process. Integrin- $\alpha 9$ and one of its ligands, Fn-ElIIIA, are required for the assembly of fibronectin and organization of the extracellular matrix core of the lymphatic valve leaflets (3), but the cellular function of ephrin-B2 in valve formation remains unknown. As observed in lymphatic valves, *Itga9*- as well as *Fn-ElIIIA*-deficient venous valves had short leaflets, suggestive of similar function. Continuous integrin- $\alpha 9$ and ephrin-B2 signaling was also found to be required for the maintenance of valves, but whereas integrin- $\alpha 9$ depletion in mature venous valves led to their regression, the morphology of lymphatic valves was not affected during the same time period. This could be because there is a higher requirement for repair of venous valves, which are exposed to harsher hemodynamic conditions compared with valves in lymphatic vessels. These results suggest that valve maintenance requires continuous synthesis and assembly of the extracellular matrix core of the leaflet and that any defects in these processes can lead to degeneration of venous and lymphatic valves.

In summary, our data identified what we believe to be the first molecular regulators of venous valves and highlighted involvement of common morphogenetic processes and signaling pathways in controlling valve formation in veins and lymphatic vessels.

Methods

Antibodies. Antibodies used for immunostaining were rabbit anti-human Prox1 (gift from T. Petrova, CePO, CHUV, and University of Lausanne, Lausanne, Switzerland), biotinylated goat anti-human Prox1 (R&D Systems), rat anti-mouse PECAM-1 (BD Biosciences – Pharmingen), hamster anti-mouse podoplanin (Developmental Studies Hybridoma Bank), goat anti-mouse integrin- $\alpha 9$ (R&D Systems), and mouse anti-human fibronectin (FN-3E2; Sigma-Aldrich). Secondary antibodies conjugated to Cy2, Cy3, or Cy5 were obtained from Jackson ImmunoResearch. Antibodies conjugated to biotin and streptavidin-alkaline phosphatase were obtained from Sigma-Aldrich.

Mice. *Itga9*^{-/-} (15) and *Itga9*^{flx} (30) mice (both provided by D. Shepard, UCSF, San Francisco, California, USA), *Fn-ElIIIA*^{-/-} mice (ref. 31; provided by A. Muro, International Centre for Genetic Engineering and Biotechnology, Trieste, Italy), *Efnb2*^{flx} mice (ref. 32; provided by R. Klein, Max-Planck-Institute of Neurobiology, Martinsried, Germany), *Efnb2*^{GFP} mice (ref. 13; provided by P. Soriano, Mount Sinai School of Medicine, New York, New York, USA), *Vegfr3*^{lacZ} mice (ref. 25, provided by K. Alitalo, University of Helsinki, Helsinki, Finland), and *Tie2*^{lacZ} mice (12) were described previously. *R26-mTmG* (14) mice were obtained from Jackson Laboratory. *Prox1-CreERT2* mice were generated using BAC transgenesis. A cDNA encoding tamoxifen-inducible Cre recombinase (CreERT², gift from P. Chambon, Institute of Genetics and Molecular and Cellular Biology, Illkirch CEDEX, Illkirch, France) followed by SV40 polyadenylation signal was introduced into the start codon of *Prox1* in BAC clone RP23-190F21 using homologous recombination in bacteria.

2 founder lines were generated by pronuclear injection and tested in combination with Cre reporter strains, followed by 4-OHT administration, for specificity and efficiency of Cre-mediated recombination. One of the founder lines gave complete recombination in all *Prox1*-expressing tissues and was used for this study. Cre-mediated recombination was induced by intraperitoneal injection of 4-OHT (2 μ l of 25 mg/ml dissolved in ethanol) at P0–P2, or tamoxifen was administered orally using Harlan Teklad CRD TAM400 diet (>3-week-old mice). All mouse experiments were approved by the United Kingdom Home Office.

Immunostaining. Skin and overlying fascia were removed from the iliac region of mice to reveal the common, external, and internal iliac veins. Blood was flushed out of the veins using a syringe filled with PBS, and the vessels were opened longitudinally along the anterior surface using either a tungsten needle and a scalpel or fine scissors. The samples were fixed in 4% PFA for 2 hours at room temperature. Whole-mount staining of the tissue was done as previously described (3). In brief, the samples were incubated for 30 minutes in blocking solution (0.3% Triton-X 100 in PBS containing 5% bovine serum albumin), followed by incubation with the primary (overnight at 4°C) and secondary antibodies (2 hours at room temperature). After washing, the samples were mounted in Mowiol and analyzed using Zeiss LSM 710 laser scanning confocal microscope. All confocal images represent 2D projections of z stacks.

Human venous valves were obtained from the long saphenous vein isolated during coronary artery bypass surgery at St. Thomas' Hospital (ethics no. 10/H0701/68, approved by East London REC 3 Research Ethics Proportionate Review Sub-Committee, London, United Kingdom). All patients provided written informed consent. Veins were dissected longitudinally under a dissecting microscope to locate valves and snap-frozen in OCT (TissueTek). Cryostat sections (7 μ m) were fixed in acetone and immunostained using biotinylated Prox1 antibodies and located with streptavidin-alkaline phosphatase complex, followed by visualization using BCIP/NBT substrate (Vector Laboratories). Sections were photographed using a Micropublisher 3.3RTV camera mounted on a Leitz DMRB microscope with PL Fluotar $\times 10$, $\times 20$, and $\times 40$ lenses (Leica).

SEM. Veins from P6 and P11 mice were fixed in 4% PFA and 2.5% glutaraldehyde in 0.1 M sodium cacodylate buffer (pH 7.4) for 2 hours at room temperature, followed by postfixation in 1% reduced osmium tetroxide and 1.5% potassium ferricyanide for 24 hours. Samples were dehydrated through an ethanol series, washed in acetone, underwent critical point drying at 1,200 psi and 32°C, and then underwent platinum coating (Polaron SC7640 Sputter Coater) for up to 6 minutes. Images in Figure 2A (stages 0 and 1) and Figures 5 and 6 were taken using a field emission scanning electron microscope (JEOL/JSM-6700F). Human veins from coronary artery bypass grafting were opened longitudinally using a dissecting microscope prior to fixation in 2.5% glutaraldehyde. Samples in for Figure 1, E, G, and I, were dried to critical point, sputter coated, and viewed in a Hitachi S-3500N scanning electron microscope.

Combined localization of β -galactosidase activity and SEM was carried out by fixing the iliac region of *Tie2*^{lacZ} mice in 5% formaldehyde and 0.8% glutaraldehyde for 30–90 minutes at 4°C, then staining using the β -gal substrate X-gal. Valves were photographed in PBS using a Nikon Coolpix 995 camera mounted on a Leica M3C dissecting microscope. Subsequent SEM analysis was carried out after longitudinal cutting open of the vein using a curved scalpel blade over an intraluminal tungsten wire, followed by further fixation of the vein in 2% glutaraldehyde and 1% formaldehyde in sodium cacodylate buffer. The vein was then dissected into blocks, osmified (1% osmium) for 24 hours on a rotator, dehydrated through alcohol, critical point dried, and sputter coated. Samples in Figure 1, D, F, H, and J and Figure 2, A (stages 2–4), D, and E were viewed in a Cambridge Stereoscan 360.



Statistics. P values were calculated using χ^2 test or 2-tailed Student's *t* test (for Figure 6O). A P value less than 0.05 was considered significant.

Acknowledgments

We thank Dean Sheppard for *Itga9* mice, Andres Muro for *Fn-ElIIIA* mice, Rüdiger Klein for *Efnb2^{lx}* mice, Kari Alitalo for *Vegfr3^{lacZ}* mice, Phil Soriano for *Efnb2^{GFP}* mice, Tatiana Petrova for Prox1 antibodies, and Pierre Chambon for *CreER^{T2}* cDNA. We also thank Ken Blight, Lucy Collinson, Ken Brady, and Fiona Winning for expert advice and help with SEM, all staff at LRI animal units and Joanna Bytnar at St George's for animal husbandry, and Sandra Webb and Ray Moss for technical advice. This work has been supported by Can-

cer Research UK (to E. Bazigou and T. Makinen), Medical Research Council (to O.T.A. Lyons), NIH Research (to O.T.A. Lyons), and British Heart Foundation (to N.A. Brown and O.T.A. Lyons).

Received for publication March 16, 2011, and accepted in revised form May 25, 2011.

Address correspondence to: Taija Makinen, Lymphatic Development Laboratory, Cancer Research UK London Research Institute, 44 Lincoln's Inn Fields, London WC2A 3LY, United Kingdom. Phone: 44.207.269.3459; Fax: 44.207.269.3147; E-mail: taija.makinen@cancer.org.uk.

1. Tammela T, Alitalo K. Lymphangiogenesis: Molecular mechanisms and future promise. *Cell*. 2010; 140(4):460–476.
2. Armstrong EJ, Bischoff J. Heart valve development: endothelial cell signaling and differentiation. *Circ Res*. 2004;95(5):459–470.
3. Bazigou E, et al. Integrin-alpha9 is required for fibronectin matrix assembly during lymphatic valve morphogenesis. *Dev Cell*. 2009;17(2):175–186.
4. Makinen T, et al. PDZ interaction site in ephrinB2 is required for the remodeling of lymphatic vasculature. *Genes Dev*. 2005;19(3):397–410.
5. Petrova TV, et al. Defective valves and abnormal mural cell recruitment underlie lymphatic vascular failure in lymphedema distichiasis. *Nat Med*. 2004;10(9):974–981.
6. Norrmen C, et al. FOXC2 controls formation and maturation of lymphatic collecting vessels through cooperation with NFATc1. *J Cell Biol*. 2009; 185(3):439–457.
7. Lim CS, Davies AH. Pathogenesis of primary varicose veins. *Br J Surg*. 2009;96(11):1231–1242.
8. Fang J, et al. Mutations in FOXC2 (MFH-1), a forkhead family transcription factor, are responsible for the hereditary lymphedema-distichiasis syndrome. *Am J Hum Genet*. 2000;67(6):1382–1388.
9. Mellor RH, et al. Mutations in FOXC2 are strongly associated with primary valve failure in veins of the lower limb. *Circulation*. 2007;115(14):1912–1920.
10. Chang CP, et al. A field of myocardial-endocardial NFAT signaling underlies heart valve morphogenesis. *Cell*. 2004;118(5):649–663.
11. Mellor RH, et al. Lymphatic dysfunction, not aplasia, underlies Milroy disease. *Microcirculation*. 2010;17(4):281–296.
12. Schlaeger TM, et al. Uniform vascular-endothelial-cell-specific gene expression in both embryonic and adult transgenic mice. *Proc Natl Acad Sci U S A*. 1997;94(7):3058–3063.
13. Davy A, Soriano P. Ephrin-B2 forward signaling regulates somite patterning and neural crest cell development. *Dev Biol*. 2007;304(1):182–193.
14. Muzumdar MD, Tasic B, Miyamichi K, Li L, Luo L. A global double-fluorescent Cre reporter mouse. *Genesis*. 2007;45(9):593–605.
15. Huang XZ, et al. Fatal bilateral chylothorax in mice lacking the integrin alpha9beta1. *Mol Cell Biol*. 2000;20(14):5208–5215.
16. Kampmeier OF, La Fleur Birch C. The origin and development of the venous valves with particular reference to the saphenous district. *Am J Anat*. 1927;38(3):451–499.
17. Caggiati A, Phillips M, Lametschwandtner A, Allegra C. Valves in small veins and venules. *Eur J Vasc Endovasc Surg*. 2006;32(4):447–452.
18. le Noble F, Fleury V, Pries A, Corvol P, Eichmann A, Reneman RS. Control of arterial branching morphogenesis in embryogenesis: go with the flow. *Cardiovasc Res*. 2005;65(3):619–628.
19. le Noble F, et al. Flow regulates arterial-venous differentiation in the chick embryo yolk sac. *Development*. 2004;131(2):361–375.
20. Yashiro K, Shiratori H, Hamada H. Haemodynamics determined by a genetic programme govern asymmetric development of the aortic arch. *Nature*. 2007;450(7167):285–288.
21. Davies PF. Hemodynamic shear stress and the endothelium in cardiovascular pathophysiology. *Nat Clin Pract Cardiovasc Med*. 2009;6(1):16–26.
22. Lee HJ, Koh GY. Shear stress activates Tie2 receptor tyrosine kinase in human endothelial cells. *Biochem Biophys Res Commun*. 2003;304(2):399–404.
23. Chlench S, et al. Regulation of Foxo-1 and the angiopoietin-2/Tie2 system by shear stress. *FEBS Lett*. 2007;581(4):673–680.
24. Wigle JT, et al. An essential role for Prox1 in the induction of the lymphatic endothelial cell phenotype. *EMBO J*. 2002;21(7):1505–1513.
25. Dumont DJ, et al. Cardiovascular failure in mouse embryos deficient in VEGF receptor-3. *Science*. 1998;282(5390):946–949.
26. Tammela T, et al. Blocking VEGFR-3 suppresses angiogenic sprouting and vascular network formation. *Nature*. 2008;454(7204):656–660.
27. Partanen TA, et al. VEGF-C and VEGF-D expression in neuroendocrine cells and their receptor, VEGFR-3, in fenestrated blood vessels in human tissues. *FASEB J*. 2000;14(13):2087–2096.
28. Johnson NC, et al. Lymphatic endothelial cell identity is reversible and its maintenance requires Prox1 activity. *Genes Dev*. 2008;22(23):3282–3291.
29. Adams RH, et al. Roles of ephrinB ligands and EphB receptors in cardiovascular development: demarcation of arterial/venous domains, vascular morphogenesis, and sprouting angiogenesis. *Genes Dev*. 1999;13(3):295–306.
30. Singh P, Chen C, Pal-Ghosh S, Stepp MA, Sheppard D, Van De Water L. Loss of integrin alpha9beta1 results in defects in proliferation, causing poor epithelialization during cutaneous wound healing. *J Invest Dermatol*. 2009;129(1):217–228.
31. Muro AF, et al. Regulated splicing of the fibronectin EDA exon is essential for proper skin wound healing and normal lifespan. *J Cell Biol*. 2003;162(1):149–160.
32. Grunwald IC, et al. Hippocampal plasticity requires postsynaptic ephrinBs. *Nat Neurosci*. 2004; 7(1):33–40.